10-9-2021

# Fourth-Order Nonlinear Distortion to the Power Spectrum of RF Amplifiers

Xianzhen Yang
*Portland State University*

Shiyu Li

Fu Li
*Portland State University*, lif@pdx.edu



## Citation Details

Yang, X., Li, S., & Li, F. (2021). Fourth-order nonlinear distortion to the power spectrum of RF amplifiers. *The Journal of Engineering*, tje2.12090. https://doi.org/10.1049/tje2.12090

Received: 21 August 2021 | Revised: 17 September 2021 | Accepted: 24 September 2021

The Journal of Engineering

DOI: 10.1049/tje2.12090

The Institution of Engineering and Technology WILEY

ORIGINAL RESEARCH PAPER

# Fourth-order nonlinear distortion to the power spectrum of RF amplifiers

**Xianzhen Yang** | **Shiyu Li** | **Fu Li**

Department of Electrical and Computer Engineering, Portland State University, Portland, Oregon, USA

**Correspondence**
Fu Li, Department of Electrical and Computer Engineering, Portland State University, 1900 SW 4th Avenue, Suite 160-10, Portland, Oregon 97207-0751, USA.
Email: lif@pdx.edu

**Funding information**
Portland State University Library's Open Access Fund

**Abstract**

Even-order intermodulation distortions are often considered easy to filter in narrowband radio frequency (RF) wireless systems because they are usually located far away from the desired passband and adjacent bands. However, even-order intermodulation distortions have recently attracted more interest with the increasing popularity of wideband RF applications. The authors' previous work was devoted to establishing the power spectrum model of second-order intermodulation distortion. Motivated by the latest efforts on RF power amplifier linearization with second-order and fourth-order intermodulation, our focus now is to establish a power spectrum model of fourth-order intermodulation distortion which can be used to discuss the fourth-order impacts on the passband and adjacent bands. Here, together with the authors' previous work on the odd-order intermodulation, a relatively comprehensive power spectrum model is presented here, including second-, third-, fourth-, and fifth-order intermodulation, which offers a broader view for spectrum planners and RF designers. With qualitative and quantitative reasoning, we further explain that higher-order (i.e., $n > 5$) IM distortions of a weakly nonlinear amplifier are indeed negligible. The experiment measurement at the end of this paper validates the spectrum model.

## 1 | INTRODUCTION

Nonlinearity in wireless communication systems usually exists in the RF front ends and is produced by nonlinear devices such as power amplifiers, low-noise amplifiers, mixers, etc. [1–3]. Nonlinear distortion is critical because it decreases the signal-to-noise ratio (SNR), and thus results in performance degradation. Therefore, behavioural modelling of nonlinear devices plays an important role in the design of linearization techniques used to overcome the effects of nonlinear distortion in wireless applications. Traditionally, only odd-order intermodulation (IM) distortions are of concern in narrowband RF systems because the even-order IM distortions are located far away from the desired passband and are easily filtered [4]. However, with the increasing deployment of wideband applications, even-order IM distortion may no longer be negligible. For example, the compensation or cancellation of the second-order IM distortion was suggested for wideband applications in long term evolution advanced (LTE-A) and fifth generation new radio (5G NR) systems [5, 6]. Additionally, a wideband inductorless low noise amplifier (LNA) was designed using a technique for canceling second-order IM products [7]. Furthermore, an exploratory effort was made to linearize the RF power amplifier by the injection of the IM2 and IM4 signals [8].

We derived a power spectrum model of the second-order IM distortion in our previous work [9]. Inspired by the recent attention regarding higher even-order IM distortions, we are now focusing on fourth-order IM distortion and its impact to the passband and adjacent bands. In this paper, a power spectrum model of fourth-order IM distortion is derived in terms of the amplifier parameters such as bandwidth, gain, intercept points, etc. We further explain from quantitative and qualitative perspectives that the higher-order (i.e., $n > 5$) IM of a weakly nonlinear amplifier is indeed negligible. Thus, a comprehensive power spectrum model up to fifth order is presented, which can be viewed as a blueprint for spectrum planners.

## 2 | POWER SPECTRUM OF FOURTH-ORDER IM

An OFDM signal in the passband centred at the carrier frequency $f_c$, as the input to the power amplifier, can be

represented as:

$$s(t) = \mathrm{Re}\left\{g(t)\, e^{j2\pi f_c t}\right\} = \tilde{s}(t)\cos\left[2\pi f_c t + \theta(t)\right] \quad (1)$$

where Re{•} denotes the real part of {•}, $g(t)$ is the complex envelope of $s(t)$, $\tilde{s}(t)$ and $\theta(t)$ are the magnitude and phase of $g(t)$, respectively. The power spectral density of $\tilde{s}(t)$ is given below [10]:

$$P_{\tilde{s}}(f) = \begin{cases} N_0/2, & |f| \le B \\ 0, & |f| > B \end{cases} \quad (2)$$

where $B$ is the bandwidth and $N_0 B$ is the power of $\tilde{s}(t)$.

Considering power spectrum only, an equivalent expression of Equation (1) can be written as [9]:

$$s(t) = \tilde{s}(t)\cos\left(2\pi f_c t\right) \quad (3)$$

Among the polynomial models for amplifiers, the Taylor series is perhaps the most used model and can be expressed as:

$$y(t) = a_1 s(t) + a_2 s^2(t) + a_3 s^3(t) + a_4 s^4(t) + a_5 s^5(t) + \cdots + a_n s^n(t) + \cdots \quad (4)$$

where $a_n$ is the Taylor coefficient of the $n$ th-order term, $s(t)$ and $y(t)$ are the input and output signals, respectively.

Now consider only fourth-order IM distortion $a_4 s^4(t)$ in Equation (4),

$$\begin{aligned} a_4 s^4(t) &= a_4\left[\tilde{s}(t)\cos\left(2\pi f_c t\right)\right]^4 \\ &= \frac{3}{4}a_4\tilde{s}^4(t) + \frac{1}{2}a_4\tilde{s}^4(t)\cos\left(4\pi f_c t\right) \\ &\quad + \frac{1}{8}a_4\tilde{s}^4(t)\cos\left(8\pi f_c t\right) \end{aligned} \quad (5)$$

We can see that the fourth-order IM distortions are located around the DC, the second-order harmonic frequency, and the fourth-order harmonic frequency. Since the DC term and the fourth-order harmonic frequency term are easily filtered, we will consider the fourth-order IM only at the second-order harmonic frequency from now on, which we define as:

$$y_4(t) \triangleq \frac{1}{2}a_4\tilde{s}^4(t)\cos\left(4\pi f_c t\right) = \tilde{y}_4(t)\cos\left(4\pi f_c t\right) \quad (6)$$

where $\tilde{y}_4(t) \triangleq a_4\tilde{s}^4(t)/2$.

Denoting the power spectrum of $\tilde{y}_4(t)$ as $P_{\tilde{y}_4}(f)$, the power spectrum $P_{y_4}(f)$ of $y_4(t)$ can be expressed as [9, 11],

$$P_{y_4}(f) = \frac{1}{4}\left[P_{\tilde{y}_4}(f - 2f_c) + P_{\tilde{y}_4}(f + 2f_c)\right] \quad (7)$$

Equation (7) is symmetric in frequency. In the real-time measurement, only the spectrum in the positive frequency range is measurable with twice the magnitude. Therefore, Equation (7) can be rewritten as:

$$P_{y_4}(f) = \frac{1}{2}P_{\tilde{y}_4}(f - 2f_c) \quad (8)$$

$P_{\tilde{y}_4}(f)$ can be calculated from the autocorrelation function $R_{\tilde{y}_4}(\tau)$ of $\tilde{y}_4(t)$ using the Wiener–Khintchine theorem:

$$P_{\tilde{y}_4}(f) = \mathcal{F}\left\{R_{\tilde{y}_4}(\tau)\right\} = \int_{-\infty}^{\infty} R_{\tilde{y}_4}(\tau)\, e^{-j2\pi f\tau} d\tau \quad (9)$$

where $\mathcal{F}\{\bullet\}$ denotes the Fourier transform of {•}. $R_{\tilde{y}_4}(\tau)$ can be calculated as:

$$R_{\tilde{y}_4}(\tau) = E\left\{\tilde{y}(t)\tilde{y}(t+\tau)\right\} = \frac{1}{4}a_4^2 E\left\{\tilde{s}^4(t)\tilde{s}^4(t+\tau)\right\} \quad (10)$$

Using Isserlis' theorem [12]:

$$E\left\{X_1 X_2 \cdots X_n\right\} = \sum_{p \in P_n^2} \prod_{\{i,j\} \in p} E\left\{X_i X_j\right\} \quad (11)$$

Equation (10) yields a massive expansion of 105 terms of the expectations. Through a lengthy simplification (the expansion and simplification are not included due to the page limit), we will derive:

$$\begin{aligned} R_{\tilde{y}_4}(\tau) &= \frac{1}{4}a_4^2 E\left\{\tilde{s}^4(t)\tilde{s}^4(t+\tau)\right\} \\ &= \frac{1}{4}a_4^2 N_0^4\left[9B^4 + 70B^2\frac{\sin^2(2\pi B\tau)}{4\pi^2\tau^2} + 26\frac{\sin^4(2\pi B\tau)}{16\pi^4\tau^4}\right] \\ &= \frac{9}{4}a_4^2 N_0^4 B^4 + \frac{70}{4}a_4^2 N_0^2 B^2 R_{\tilde{s}}^2(\tau) + \frac{26}{4}a_4^2 R_{\tilde{s}}^4(\tau) \end{aligned} \quad (12)$$

where $R_{\tilde{s}}(\tau) = F^{-1}\{P_{\tilde{s}}(f)\} = N_0 B\frac{\sin(2\pi B\tau)}{2\pi B\tau}$ is obtained from Equation (2).

Then, the power spectrum $P_{y_4}(f)$ can be calculated as:

$$\begin{aligned} P_{y_4}(f) &= F\left\{R_{\tilde{y}_4}(\tau)\right\} = \frac{9}{4}F\left\{a_4^2 N_0^4 B^4\right\} \\ &\quad + \frac{35}{2}a_4^2 N_0^2 B^2 F\left\{R_{\tilde{s}}^2(\tau)\right\} + \frac{13}{2}a_4^2 F\left\{R_{\tilde{s}}^4(\tau)\right\} \end{aligned} \quad (13)$$

Using convolution property of Fourier transform, $F\{R_{\tilde{s}}^2(\tau)\}$ in Equation (13) can be expressed as:

$$F\left\{R_{\tilde{s}}^2(\tau)\right\} = F\left\{R_{\tilde{s}}(\tau)\right\} \otimes F\left\{R_{\tilde{s}}(\tau)\right\} \quad (14)$$

where $\otimes$ indicates convolution. Noting $F\{R_{\tilde{s}}(\tau)\} = P_{\tilde{s}}(f)$ is given in Equation (2), Equation (14) can be calculated as:

$$F\left\{R_{\tilde{s}}^2(\tau)\right\} = \frac{N_0^2}{4}\left(2B - |f|\right), \quad |f| \le 2B \quad (15)$$

$F\{R_{\tilde{s}}^4(\tau)\}$ in Equation (13) can be derived as (see Appendix A)

$$F\left\{R_{\tilde{s}}^4(\tau)\right\} = F\left\{R_{\tilde{s}}^2(\tau)\right\} \otimes F\left\{R_{\tilde{s}}^2(\tau)\right\}$$
$$= \begin{cases} \frac{N_0^4}{16}\left(\frac{1}{2}|f|^3 - 2B|f|^2 + \frac{16}{3}B^3\right), & |f| \le 2B \\ \frac{N_0^4}{16}\left(-\frac{1}{6}|f|^3 + 2B|f|^2 - 8B^2|f| + \frac{32}{3}B^3\right), & 2B \le |f| \le 4B \end{cases} \quad (16)$$

To express Equation (17) using $G$ and fourth-order intercept point $IP_4$, $a_4^2$ can be obtained as (see Appendix B)

$$a_4^2 = \frac{2}{9}10^{\frac{2G}{5} - \frac{3IP_4}{10}} \quad (19)$$

Therefore, the final power spectrum expression of the fourth-order IM is given as:

$$P_{y_4}(f) = \begin{cases} 4P_0^4 10^{\frac{-3IP_4}{10}}\delta(f - 2f_c) + \frac{16}{9}\frac{P_0^4}{B^4}10^{\frac{-3IP_4}{10}}\left(\frac{13}{64}|f - 2f_c|^3 - \frac{13}{16}B|f - 2f_c|^2 - \frac{35}{8}B^2|f - 2f_c| + \frac{131}{12}B^3\right), & |f - 2f_c| \le 2B \\ \frac{13}{108}\frac{P_0^4}{B^4}10^{\frac{-3IP_4}{10}}\left(-|f - 2f_c|^3 + 12B|f - 2f_c|^2 - 48B^2|f - 2f_c| + 64B^3\right), & 2B \le |f - 2f_c| \le 4B \end{cases} \quad (20)$$

By substituting Equations (15) and (16) into Equation (13), Equation (13) can be expressed as:

$$P_{y_4}(f) = \begin{cases} \frac{9}{4}a_4^2N_0^4B^4\delta(f) + a_4^2N_0^4 \\ \quad \times\left(\frac{13}{64}|f|^3 - \frac{13}{16}B|f|^2\right. \\ \quad \left. - \frac{35}{8}B^2|f| + \frac{131}{12}B^3\right), & |f| \le 2B \\ \frac{13}{192}a_4^2N_0^4\left(-|f|^3 + 12B|f|^2\right. \\ \quad \left. - 48B^2|f| + 64B^3\right), & 2B \le |f| \le 4B \end{cases} \quad (17)$$

Substitute Equation (17) into Equation (8), the power spectrum of fourth-order IM can be obtained as:

$$P_{y_4}(f) = \begin{cases} \frac{9}{8}a_4^2N_0^4B^4\delta(f - 2f_c) \\ \quad + \frac{1}{2}a_4^2N_0^4\left(\frac{13}{64}|f - 2f_c|^3\right. \\ \quad - \frac{13}{16}B|f - 2f_c|^2 - \frac{35}{8}B^2 \\ \quad \left.|f - 2f_c| + \frac{131}{12}B^3\right), & |f - 2f_c| \le 2B \\ \frac{13}{384}a_4^2N_0^4\left(-|f - 2f_c|^3\right. \\ \quad + 12B|f - 2f_c|^2 - 48B^2 \\ \quad \left.|f - 2f_c| + 64B^3\right), & 2B \le |f - 2f_c| \le 4B \end{cases} \quad (18)$$

where $P_0 = a_1^2N_0B/2$ is the power of the linear output.

An interesting observation can be made from Equation (20), the frequency spread of the fourth-order IM around second harmonic $2f_c$ is twice as wide as that of the second-order IM at $2f_c$ [9]. This is because the Fourier transform of the fourth power to the autocorrelation $F\{R_{\tilde{s}}^4(\tau)\}$ in Equation (15) can be further decomposed as a four-time convolution of $F\{R_{\tilde{s}}(\tau)\}$, i.e., $F\{R_{\tilde{s}}^4(\tau)\} = F\{R_{\tilde{s}}^2(\tau)\} \otimes F\{R_{\tilde{s}}^2(\tau)\} = F\{R_{\tilde{s}}(\tau)\} \otimes F\{R_{\tilde{s}}(\tau)\} \otimes F\{R_{\tilde{s}}(\tau)\} \otimes F\{R_{\tilde{s}}(\tau)\}$. Since each $F\{R_{\tilde{s}}(\tau)\}$ has a frequency spread of $2B$, the frequency spread of the fourth-order IM is $8B$. This is not only true at $2f_c$, but also at the fourth-order harmonic $4f_c$. However, the spread is $nB$ at DC if we consider only the positive frequency, but it is symmetric in negative frequency.

From these observations, an important insight can be made: since the $n$th even-order involves the calculation of $F\{R_{\tilde{s}}^n(\tau)\}$, we could conclude that the frequency spread of the $n$th even-order IM is $2nB$, except at DC, where it is $nB$.

The Power spectrum of fourth-order IM is illustrated in Figure 1.

## 3 | A COMPREHENSIVE POWER SPECTRUM MODEL UP TO FIFTH ORDER

Historically, the power spectrum model of the PA nonlinearity includes only the third-order IM [13]. In later experiments and analyses, it was discovered that considering only the third-order IM is not accurate enough to describe the nonlinearity; thus, the fifth-order IM was included in the power spectrum model, in our previous work [10]. This power spectrum model with the third- and fifth- order IM around the passband is given below:

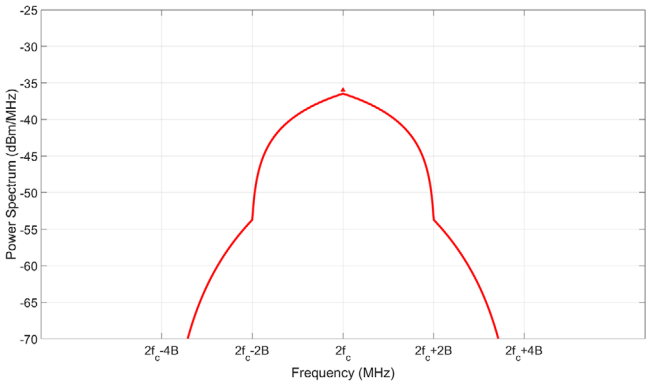


**FIGURE 1** Power spectrum of $P_{y_4}(f)$

The power spectrum model of second-order IM can be obtained from [9] as,

$$P_{y_2}(f)=\begin{cases}\frac{1}{4}P_0^2 10^{-\frac{IP_2}{10}}\delta\left(f-2f_c\right)\\ \quad+\frac{1}{8B^2}P_0^2 10^{-\frac{IP_2}{10}}\\ \quad\times\left(2B-\left|f-2f_c\right|\right), & \left|f-2f_c\right|\le 2B\\ 0, & \left|f-2f_c\right|>2B\end{cases} \tag{22}$$

The IM terms higher than the fourth- and fifth- order are much less significant, and are generally considered negligible by technology developers. This could be intuitively explained as below:

1. As observed from the Taylor series Equation (4), the higher-order terms carry less energy when the power amplifier is weakly nonlinear, otherwise the amplifier should be simply discarded.

$$P_{y_{135}}(f)=\begin{cases}\frac{1}{2B}\left[P_0-6P_0^2 10^{-\frac{IP_3}{10}}-30P_0^3 10^{-\frac{IP_5}{5}}+9P_0^3 10^{-\frac{IP_3}{5}}+90P_0^4 10^{-\frac{IP_3}{10}-\frac{IP_5}{5}}+225P_0^5 10^{-\frac{2IP_5}{5}}\right]\\ +\frac{1}{8B^3}\left[6P_0^3 10^{-\frac{IP_3}{5}}+120P_0^4 10^{-\frac{IP_3}{10}-\frac{IP_5}{5}}+150P_0^5 10^{-\frac{2IP_5}{5}}\right]\left[3B^2-\left|f-f_c\right|^2\right] & \left|f-f_c\right|\le B\\ +\frac{10}{32}\frac{P_0^5}{B^5}10^{-\frac{2IP_5}{5}}\left\{3\left[5B^2-\left|f-f_c\right|^2\right]^2+40B^4\right\},\\ \frac{1}{16B^3}\left[6P_0^3 10^{-\frac{IP_3}{5}}+120P_0^4 10^{-\frac{IP_3}{10}-\frac{IP_5}{5}}+150P_0^5 10^{-\frac{2IP_5}{5}}\right]\left(3B-\left|f-f_c\right|\right)^2 & B\ge\left|f-f_c\right|\le 3B\\ +\frac{10}{16}\frac{P_0^5}{B^5}10^{-\frac{2IP_5}{5}}\left[2B\left(4B-\left|f-f_c\right|\right)^3+2B^3\left(4B-\left|f-f_c\right|\right)-\left(3B-\left|f-f_c\right|\right)^4\right],\\ \frac{5}{32}\frac{P_0^5}{B^5}10^{-\frac{2IP_5}{5}}\left(5B-\left|f-f_c\right|\right)^4, & 3B\ge\left|f-f_c\right|\le 5B\\ 0, & \left|f-f_c\right|>5B\end{cases} \tag{21}$$

From Equation (21), we notice that the frequency spread of the third-order IM is $6B$ and that of the fifth-order IM is $10B$, as they are also calculated from $F\{R_s^n(\tau)\}$, when $n$ equals 3 and 5, respectively. Together with the discussion of the even-order IM earlier, we could now draw a general conclusion. The frequency spread of the $n$th-order IM is $2nB$, regardless of whether $n$ is even or odd; this may occur at any frequency location, except it would be $nB$ around the DC when $n$ is even.

2. Using the trigonometric property, it is easy to show the higher-order terms $a_n s^n(t)$ will have $\left\lceil\frac{n+1}{2}\right\rceil$ distinct frequency segments as,

$$\begin{aligned}a_n s^n(t)&=a_n\left[\tilde{s}(t)\cos\left(2\pi f_c t\right)\right]^n=a_n\tilde{s}^n(t)\left[\cos\left(2\pi f_c t\right)\right]^n\\&=a_n\tilde{s}^n(t)\frac{1}{2^n}\sum_{k=0}^{n}\binom{n}{k}\cos\left[2\pi(n-2k)f_c t\right]\end{aligned} \tag{23}$$

where $\lceil x \rceil$ denotes the ceiling function, which maps $x$ to the least integer greater than or equal to $x$.

3. At each segment, the frequency spread of higher-order IM would be broader as it is $2nB$, ($nB$ at DC for even order) thus the power spectrum of higher-order IM will be distributed over a wider spread.

With all the reasons above, the power spectrum of higher-order terms will generally have much lower value. Hence, the power spectrum impacts of all higher-order terms are often ignored, which also concurs with the practice of the designers.

Therefore, a relatively comprehensive (up to the fifth order) power spectrum model, concerning passband and adjacent frequency range till second harmonic, can be expressed as:

$$P_y(f) = P_{y135}(f) + P_{y2}(f) + P_{y4}(f)$$

$$= \begin{cases} \frac{1}{2B}\left[P_0 - 6P_0^2 10^{-\frac{IP_3}{10}} - 30P_0^3 10^{-\frac{IP_5}{5}} + 9P_0^3 10^{-\frac{IP_3}{5}} + 90P_0^4 10^{-\frac{IP_3}{10}-\frac{IP_5}{5}} + 225P_0^5 10^{-\frac{2IP_5}{5}}\right] \\ +\frac{1}{8B^3}\left[6P_0^3 10^{-\frac{IP_3}{5}} + 120P_0^4 10^{-\frac{IP_3}{10}-\frac{IP_5}{5}} + 150P_0^5 10^{-\frac{2IP_5}{5}}\right]\left[3B^2 - |f-f_c|^2\right] & |f-f_c| \le B \\ +\frac{10}{32}\frac{P_0^5}{B^5}10^{-\frac{2IP_5}{5}}\left\{3\left[5B^2 - |f-f_c|^2\right]^2 + 40B^4\right\}, \\ \\ \frac{1}{16B^3}\left[6P_0^3 10^{-\frac{IP_3}{5}} + 120P_0^4 10^{-\frac{IP_3}{10}-\frac{IP_5}{5}} + 150P_0^5 10^{-\frac{2IP_5}{5}}\right]\left(3B - |f-f_c|\right)^2 & B < |f-f_c| \le 3B \\ +\frac{10}{16}\frac{P_0^5}{B^5}10^{-\frac{2IP_5}{5}}\left[2B\left(4B - |f-f_c|\right)^3 + 2B^3\left(4B - |f-f_c|\right) - \left(3B - |f-f_c|\right)^4\right], \\ \\ \frac{5}{32}\frac{P_0^5}{B^5}10^{-\frac{2IP_5}{5}}\left(5B - |f-f_c|\right)^4, & 3B < |f-f_c| \le 5B \\ \\ \left(4P_0^4 10^{\frac{-3IP_4}{10}} + \frac{1}{4}P_0^2 10^{\frac{-IP_2}{10}}\right)\delta(f-2f_c) + \frac{16}{9}\frac{P_0^4}{B^4}10^{\frac{-3IP_4}{10}}\left(\frac{13}{64}|f-2f_c|^3 - \frac{13}{16}B|f-2f_c|^2\right) \\ -\left(\frac{70}{9}\frac{P_0^4}{B^2}10^{\frac{-3IP_4}{10}} + \frac{P_0^2}{8B^3}10^{\frac{-IP_2}{10}}\right)|f-2f_c| + \frac{524}{27}\frac{P_0^4}{B}10^{\frac{-3IP_4}{10}} + \frac{P_0^2}{4B}10^{\frac{-IP_2}{10}}, & |f-2f_c| \le 2B \\ \\ \frac{13}{108}\frac{P_0^4}{B^4}10^{\frac{-3IP_4}{10}}\left(-|f-2f_c|^3 + 12B|f-2f_c|^2 - 48B^2|f-2f_c| + 64B^3\right), & 2B \le |f-2f_c| \le 4B \\ \\ 0, \text{otherwise} \end{cases} \tag{24}$$

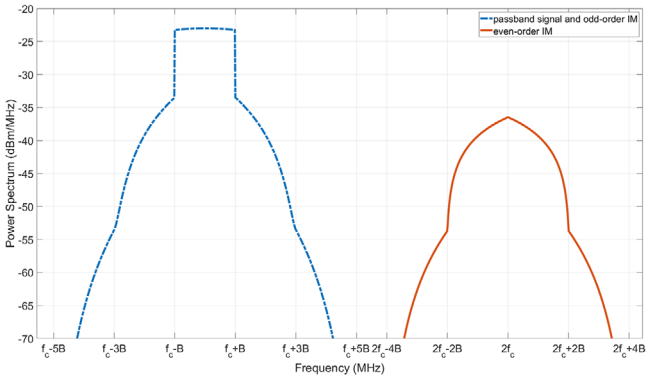


**FIGURE 2** Power spectrum of $P_y(f)$

This comprehensive power spectrum model Equation (23) is illustrated in Figure 2.

In Equation (24), the first three frequency segments, all centred around the carrier frequency $f_c$, are the passband signal and third- and fifth- order IM distortions; the next two segments, centred around the second-order harmonic frequency $2f_c$, are second- and fourth- order IM distortions. Therefore, we can separate Equation (24) into two parts, based on the two centre frequencies above.

$$P_y(f) = P_{y_{135}}(f) + P_{y_{24}}(f) \tag{25}$$

$P_{y_{135}}(f)$ represents the passband signal and odd-order IM (up to the fifth), and $P_{y_{24}}(f)$ represents the even-order IM (up to the fourth). The expression of $P_{y_{24}}(f)$ is the summation of Equations (20) and (22), which is given below:

$$P_{y_{24}}(f) = P_{y_2}(f) + P_{y_4}(f)$$

$$= \begin{cases} \left(9P_0^4 10^{\frac{-3IP_4}{10}} + \frac{1}{4}P_0^2 10^{\frac{-IP_2}{10}}\right)\delta(f-2f_c) + \frac{1}{4}\frac{P_0^4}{B^4}10^{\frac{-3IP_4}{10}}\left(\frac{13}{64}|f-2f_c|^3 - \frac{13}{16}B|f-2f_c|^2\right) & \\ -\left(\frac{35}{32}\frac{P_0^4}{B^2}10^{\frac{-3IP_4}{10}} + \frac{P_0^2}{8B^3}10^{\frac{-IP_2}{10}}\right)|f-2f_c| + \frac{131}{48}\frac{P_0^4}{B}10^{\frac{-3IP_4}{10}} + \frac{P_0^2}{4B^2}10^{\frac{-IP_2}{10}}, & |f-2f_c| \le 2B \\ \frac{13}{48}\frac{P_0^4}{B^4}10^{\frac{-3IP_4}{10}}\left(-|f-2f_c|^3 + 12B|f-2f_c|^2 - 48B^2|f-2f_c| + 64B^3\right), & 2B \le |f-2f_c| \le 4B \end{cases} \tag{26}$$

In Figure 2, $P_{y_{135}}(f)$ is shown as the blue dash-dot (for black-and-white print) curve and $P_{y_{24}}(f)$ is shown as the red curve. We notice that if the bandwidth increases relative to the carrier frequency, the even-order IM might interfere with the passband and adjacent bands. Therefore, several frequency scenarios will be discussed in terms of the relationship between the bandwidth and carrier frequency.

## 4 | FREQUENCY SCENARIOS BETWEEN EVEN- AND ODD- ORDER INTERMODULATION

From Equations (21) and (26), we can see that the even-order IM (up to the fourth) is located in the frequency range from $(2f_c - 4B)$ to $(2f_c + 4B)$, while the passband and odd-order IM (up to fifth) are located in the frequency range from $(f_c - 5B)$ to $(f_c + 5B)$. The impact of the even-order IM to the passband and adjacent bands will be discussed in three frequency scenarios in terms of the relationship between carrier frequency $f_c$ and bandwidth $B$.

### 4.1 | Frequency scenario 1

$$f_c > 9B \tag{27}$$

The inequality in Equation (27) is from $(2f_c - 4B) > (f_c + 5B)$. As shown in Figure 2, the left edge of the even-order IM $(2f_c - 4B)$ does not reach the right edge of the odd-order IM $(f_c + 5B)$. In other words, there is no overlap between the even-order IM and the odd-order IM. This would likely be the most common situation in RF wireless communications. In fact, the centre frequency is usually far greater than the bandwidth $(f_c \gg 9B)$. While in Scenario 1, the even-order IM may not be able to overlap with the passband and immediate adjacent bands (located at odd-order IM) directly, it can affect other bands relatively far away from the desired passband. For example, assume a 5G signal is transmitted at 940 MHz with a bandwidth of $B = 20$MHz (in downlink band n8 [14]); the even-order IM at the second harmonic will locate around 1880 MHz with a frequency spread of $8B = 160$MHz, which will cover downlink bands n2 and n3. Since we are considering the fourth-order IM, whose spread is twice that of the second-order IM, it may affect wider frequency ranges than if considering the second-order IM only.

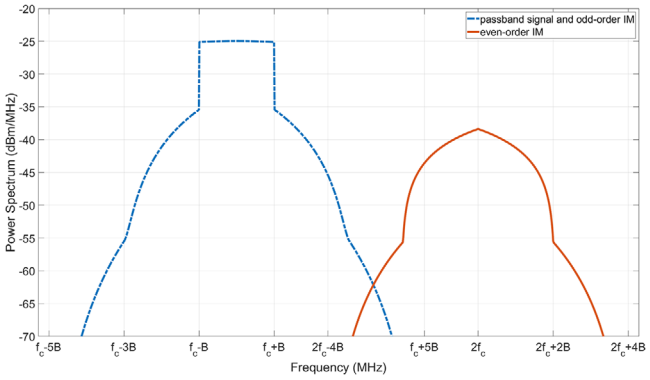


**FIGURE 3** Power spectrum of passband signal, odd-order IM, and even-order IM in Scenario 2

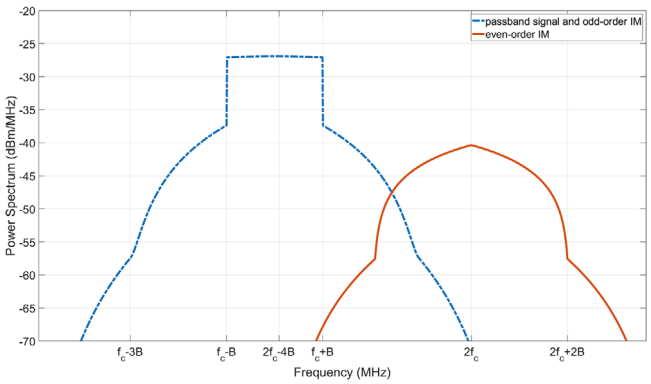


**FIGURE 4** Power spectrum of passband signal, odd-order IM, and even-order IM in Scenario 3

## 4.2 | Frequency scenario 2

$$5B < f_c \leq 9B \tag{28}$$

This inequality in Equation (28) is from $(f_c + B) < (2f_c - 4B) \leq (f_c + 5B)$. This hypothetical scenario might occur in wideband applications other than 5G. As shown in Figure 3, the left edge of the even-order IM $(2f_c - 4B)$ falls into the odd-order IM but has not touched the passband yet. This means the even-order IM has affected the odd-order IM but there is no overlap between the even-order IM and passband signal. In this situation, the adjacent channel power ratio (ACPR) performance is degraded because the adjacent power is increased by the even-order IM. The even-order IM also brings new challenges to linearization technology. As in case of this scenario, it is not easily filtered.

## 4.3 | Frequency scenario 3

$$f_c \leq 5B \tag{29}$$

This condition is from $(f_c + B) > (2f_c - 4B)$. As shown in Figure 4, the left edge of the even-order IM $(2f_c - 4B)$ has fallen into the desired passband. However, this situation is unlikely to happen in current wireless communications, as few applications can satisfy the inequality.

From the scenarios mentioned above, bandpass or bandstop filters could be used to remove the even-order IM distortion in Scenario 1, and predistortion techniques could be applied to avoid the even-order IM in Scenarios 2 and 3.

# 5 | EXPERIMENT VALIDATION

The experiment setup is shown in Figure 5. An Agilent E4438 ESG vector signal generator is used to transmit an OFDM signal through a Mini-Circuit amplifier ZX60-8008E+. A Tektronix RSA 6120A real-time spectrum analyser is used to detect the amplified signal from the output of the amplifier. A Tektronix PS2520G DC power supply provides power for the amplifier.

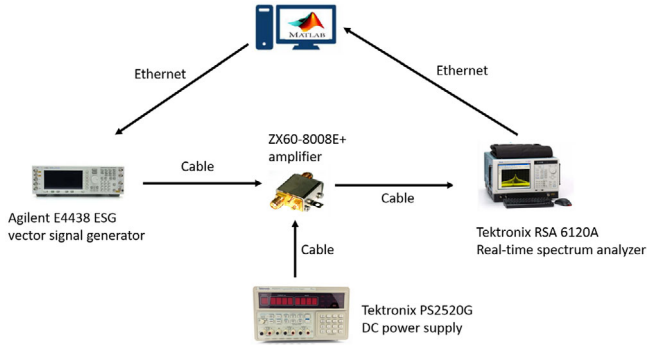


**FIGURE 5** Experiment setup

In this experiment, the centre frequency of the OFDM signal is set at $f_c = 940$MHz with a bandwidth $B = 20$MHz. These parameters are chosen from 5G NR frequency bands and channel bandwidth [14]. The $IP_2$ and $IP_4$ are measured as 38.69 and 39.31 dBm, respectively, using a two-tone test at the same centre frequency [15]. The power of the linear output $P_0$ is $-5.9$ dBm. By observation from the spectrum analyser, we can see that the power spectrum of the even-order IM is located around the second-order harmonic frequency as expected. The measured and predicted power spectrum of the even-order IM is shown in Figure 6. In Figure 6, the blue waveform represents the power spectrum of measured even-order IM, and the red curve represents the power spectrum of predicted even-order IM. Note that the noise floor detected in the experiment was added in the predicted power spectrum of the even-order IM.

# 6 | CONCLUDING REMARKS

In this paper, we developed a power spectrum model for the fourth-order IM distortion in terms of amplifier parameters, such as bandwidth, gain, and the fourth-order intercept point.

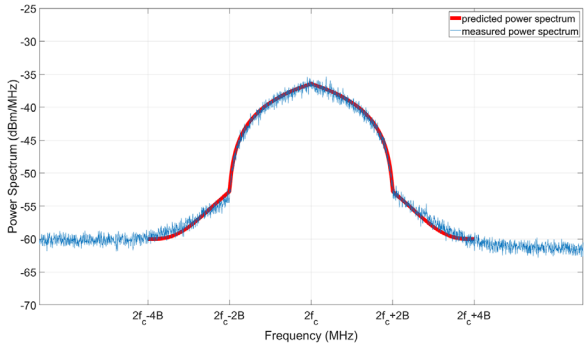


**FIGURE 6** Measured and predicted power spectrum of even-order IM

Combining this fourth-order spectrum model with our previous work, consisting of power spectrum models for passband signal, second-, third-, and fifth- order IM, we have provided a comprehensive power spectrum model up to the fifth order, denoting an overall spectrum view which will benefit designers and planners. Through the derivation, we illustrate the feasibility of neglecting higher-order IM distortions with respect to power spectrum models.

## FUNDING

Publication of this article in an open access journal was funded by the Portland State University Library's Open Access Fund.

## CONFLICT OF INTEREST

The authors declare that they have no conflicts of interest.

## ORCID

*Fu Li* https://orcid.org/0000-0001-8819-0547

## REFERENCES

1. Gharaibeh, K.M.: Nonlinear Distortion in Wireless Systems: Modeling and Simulation with MATLAB. IEEE Press, Piscataway, NJ (2012)
2. Mohammadi, S.M.: A New Design Approach of Low-Noise Stable Broadband Microwave Amplifier Using Hybrid Optimization Method. IETE Journal of Research. 1–7 (2020). https://www.tandfonline.com/doi/citedby/10.1080/03772063.2020.1787879?scroll=top&needAccess=true
3. Iqbal, A., Jiat Tiang, J., Kin Wong, S., Alibakhshikenari, M., Falcone, F., Limiti, E.: Multimode HMSIW-based bandpass filter with improved selectivity for fifth-generation (5G) RF front-ends. Sensors 20(24), 7320 (2020)
4. Cripps, S.C.: RF Power Amplifiers for Wireless Communications, 2nd ed., Artech House, Boston (2006)
5. Chen, H.-H., Huang, P.-C., Wen, C.-K., Chen, J.-T.: Adaptive compensation of even-order distortion in direct conversion receivers. In: 2003 IEEE 58th Vehicular Technology Conference. VTC 2003-Fall (IEEE Cat. No.03CH37484), Orlando, FL, pp. 271–274 (2003)
6. Gebhard, A., et al.: A robust nonlinear RLS type adaptive filter for second-order-intermodulation distortion cancellation in FDD LTE and 5G direct conversion transceivers. IEEE Trans. Microw. Theory Tech. 67(5), 1946–1961 (2019)
7. Arnborg, T., Alvandpour, A.: Wideband inductorless LNA employing simultaneous 2nd and 3rd order distortion cancellation. In: NORCHIP 2010, Tampere, Finland, pp. 1–4 (2010)
8. Đorić, A., Atanasković, A. & Ilić, N.M. : Linearization and efficiency enhancement of the RF power amplifier by the even-order nonlinear signal injection. In: 2015 12th International Conference on Telecommunication in Modern Satellite, Cable and Broadcasting Services (SIKS), Nis, Serbia, pp. 106–109 (2015)
9. Yang, X., Li, S., Yan, S., Li, F.: On IP2 impact to nonlinear distortion of RF amplifiers. J. Eng. 2021(4), 209–215 (2021)
10. Liu, C., Xiao, H., Wu, Q., Li, F.: Spectrum design of RF power amplifier for wireless communication systems. IEEE Trans. Consum. Electron. 48(1), 72–80 (2002)
11. Couch, L.W.: Digital and Analog Communication Systems, 8th ed., Pearson, Upper Saddle River, NJ (2013)
12. Isserlis, L.: On a formula for the product-moment coefficient of any order of a normal frequency distribution in any number of variables. Biometrika 12(1–2), 134–139 (1918)
13. Wu, Q., Testa, M., Larkin, R.: Linear RF power amplifier design for CDMA signals. In: 1996 IEEE MTT-S International Microwave Symposium Digest, San Francisco, CA, pp. 851–854 (1996)
14. 3GPP specification series: 38series.: https://www.3gpp.org/DynaReport/38-series.htm (2021). Accessed 07 August 2021
15. Measuring the nonlinearities of RF amplifiers using signal generators and a spectrum analyzer. https://scdn.rohde-schwarz.com/ur/pws/dl_downloads/dl_application/application_notes/1ma71/1MA71_2e_amplifier_nonlin_meas.pdf (2021). Accessed 16 September 2021

**How to cite this article:** Yang, X., Li, S., Li, F.: Fourth-order nonlinear distortion to the power spectrum of RF amplifiers. J. Eng. 1–11 (2021). https://doi.org/10.1049/tje2.12090

## APPENDIX A

Derivation of $F\{R_{\tilde{s}}^4(\tau)\}$.

As the Fourier transform is symmetric with zero frequency, we will only provide the derivation along the positive frequency as below.

When $2B \le f \le 4B$,

$$F\left\{R_{\tilde{s}}^4(\tau)\right\} = \int_{f-2B}^{2B} \left[\frac{N_0^2}{4}(2B-\tau)\right]\left[\frac{N_0^2}{4}(2B-f+\tau)\right] d\tau$$

$$= \int_{f-2B}^{2B} \frac{N_0^4}{16}(4B^2 - 2Bf + 2B\tau - 2B\tau + f\tau - \tau^2) d\tau$$

$$= \frac{N_0^4}{16}\left[4B^2\tau - 2Bf\tau + \frac{1}{2}f\tau^2 - \frac{1}{3}\tau^3\right]_{f-2B}^{2B}$$

$$= \frac{N_0^4}{16}\Big[4B^2(2B-(f-2B)) - 2Bf(2B-(f-2B))$$

$$+ \frac{1}{2}f\left(4B^2 - \left(f-2B\right)^2\right) - \frac{1}{3}\left(8B^3 - \left(f-2B\right)^3\right)\Big]$$

$$= \frac{N_0^4}{16}\Big[4B^2(4B-f) - 2Bf(4B-f)$$

$$+ \frac{1}{2}f(4B^2 - f^2 - 4B^2 + 4Bf) - \frac{1}{3}(8B^3$$

$$
\begin{aligned}
&- (f^3 - 6Bf^2 + 12B^2 f - 8B^3))\Big] \\
&= \frac{N_0^4}{16}\Big(16B^3 - 4B^2 f - 8B^2 f + 2Bf^2 + 2B^2 f \\
&- \frac{1}{2}f^3 - 2B^2 f + 2Bf^2 - \frac{8}{3}B^3 + \frac{1}{3}f^3 \\
&- 2Bf^2 + 4B^2 f - \frac{8}{3}B^3\Big) \\
&= \frac{N_0^4}{16}\left(-\frac{1}{6}f^3 + 2Bf^2 - 8B^2 f + \frac{32}{3}B^3\right) \qquad \text{(A1)}
\end{aligned}
$$

When $0 \le f \le 2B$,

$$
\begin{aligned}
&F\left\{R_s^4(\tau)\right\} \\
&= \int_{f-2B}^{0}\left[\frac{N_0^2}{4}(2B+\tau)\right]\left[\frac{N_0^2}{4}\left(2B-f+\tau\right)\right]d\tau \\
&+ \int_{0}^{f}\left[\frac{N_0^2}{4}(2B-\tau)\right]\left[\frac{N_0^2}{4}\left(2B-f+\tau\right)\right]d\tau \\
&+ \int_{f}^{2B}\left[\frac{N_0^2}{4}(2B-\tau)\right]\left[\frac{N_0^2}{4}\left(2B+f-\tau\right)\right]d\tau \\
&= \int_{f-2B}^{0}\frac{N_0^4}{16}\left(4B^2 - 2Bf + 2B\tau + 2B\tau - f\tau + \tau^2\right)d\tau \\
&+ \int_{0}^{f}\frac{N_0^4}{16}\left(4B^2 - 2Bf + 2B\tau - 2B\tau + f\tau - \tau^2\right)d\tau \\
&+ \int_{f}^{2B}\frac{N_0^4}{16}\left(4B^2 + 2Bf - 2B\tau - 2B\tau - f\tau + \tau^2\right)d\tau \\
&= \frac{N_0^4}{16}\left[4B^2\tau - 2Bf\tau + 2B\tau^2 - \frac{1}{2}f\tau^2 + \frac{1}{3}\tau^3\right]_{f-2B}^{0} \\
&+ \frac{N_0^4}{16}\left[4B^2\tau - 2Bf\tau + \frac{1}{2}f\tau^2 - \frac{1}{3}\tau^3\right]_{0}^{f} \\
&+ \frac{N_0^4}{16}\left[4B^2\tau + 2Bf\tau - 2B\tau^2 - \frac{1}{2}f\tau^2 + \frac{1}{3}\tau^3\right]_{f}^{2B} \\
&= \frac{N_0^4}{16}\Bigg[-\Big(4B^2(f-2B) - 2Bf(f-2B) + 2B(f-2B)^2 \\
&- \frac{1}{2}f(f-2B)^2 + \frac{1}{3}(f-2B)^3\Big)\Bigg] + \frac{N_0^4}{16} \\
&\times\left[4B^2 f - 2Bf^2 + \frac{1}{2}f^3 - \frac{1}{3}f^3\right] + \frac{N_0^4}{16} \\
&\times\Big[4B^2(2B-f) + 2Bf(2B-f) - 2B(4B^2 - f^2) \\
&- \frac{1}{2}f(4B^2 - f^2) + \frac{1}{3}(8B^3 - f^3)\Big] \\
&= -\frac{N_0^4}{16}\Big(4B^2 f - 8B^3 - 2Bf^2 + 4B^2 f \\
&+ 2B(f^2 + 4B^2 - 4Bf) - \frac{1}{2}f(f^2 - 4Bf + 4B^2) \\
&+ \frac{1}{3}(f^3 - 6Bf^2 + 12B^2 f - 8B^3)\Big) \\
&+ \frac{N_0^4}{16}\left(\frac{1}{6}f^3 - 2Bf^2 + 4B^2 f\right) \\
&+ \frac{N_0^4}{16}\Big[8B^3 - 4B^2 f + 4B^2 f - 2Bf^2 - 8B^3 + 2Bf^2 \\
&- 2B^2 f + \frac{1}{2}f^3 + \frac{8}{3}B^3 - \frac{1}{3}f^3\Big] \\
&= -\frac{N_0^4}{16}\Big(8B^2 f - 8B^3 - 2Bf^2 + 2Bf^2 + 8B^3 - 8B^2 f \\
&- \frac{1}{2}f^3 + 2Bf^2 - 2B^2 f + \frac{1}{3}f^3 - 2Bf^2 + 4B^2 f - \frac{8}{3}B^3\Big) \\
&+ \frac{N_0^4}{16}\left(\frac{1}{6}f^3 - 2Bf^2 + 4B^2 f\right) + \frac{N_0^4}{16} \\
&\times\Big[8B^3 - 2Bf^2 - 8B^3 + 2Bf^2 - 2B^2 f + \frac{1}{6}f^3 + \frac{8}{3}B^3\Big] \\
&= -\frac{N_0^4}{16}\left(-\frac{1}{6}f^3 + 2B^2 f - \frac{8}{3}B^3\right) + \frac{N_0^4}{16} \\
&\times\left(\frac{1}{6}f^3 - 2Bf^2 + 4B^2 f\right) + \frac{N_0^4}{16}\left(\frac{1}{6}f^3 - 2B^2 f + \frac{8}{3}B^3\right) \\
&= \frac{N_0^4}{16}\left(\frac{1}{2}f^3 - 2Bf^2 + \frac{16}{3}B^3\right) \qquad \text{(A2)}
\end{aligned}
$$

The derivations along the negative frequencies are similar. When $-2B \le f \le 0$,

$$
\begin{aligned}
F\left\{R_s^4(\tau)\right\} &= \int_{-2B}^{f}\left[\frac{N_0^2}{4}(2B+\tau)\right]\left[\frac{N_0^2}{4}\left(2B-f+\tau\right)\right]d\tau \\
&+ \int_{f}^{0}\left[\frac{N_0^2}{4}(2B+\tau)\right]\left[\frac{N_0^2}{4}\left(2B+f-\tau\right)\right]d\tau
\end{aligned}
$$

$$+\int_{0}^{f+2B}\left[\frac{N_0^2}{4}(2B-\tau)\right]\left[\frac{N_0^2}{4}(2B+f-\tau)\right]d\tau$$

$$=\frac{N_0^4}{16}\left(-\frac{1}{2}f^3-2Bf^2+\frac{16}{3}B^3\right) \quad \text{(A3)}$$

When $-4B \le f \le -2B$,

$$F\left\{R_{\tilde{s}}^4(\tau)\right\}=\int_{-2B}^{f+2B}\left[\frac{N_0^2}{4}(2B+\tau)\right]\left[\frac{N_0^2}{4}(2B+f-\tau)\right]d\tau$$

$$=\frac{N_0^4}{16}\left(\frac{1}{6}f^3+2Bf^2+8B^2f+\frac{32}{3}B^3\right) \quad \text{(A4)}$$

## APPENDIX B

Expression of $a_4^2$ in terms of $G$ and $IP_4$.

Consider in a two-tone test, the two tones are located at $f_1$ and $f_2$, respectively. $IP_4$ is defined as the output power level at which the output power $P_{2(f_1+f_2)}$ at the frequency $2(f_1+f_2)$ would intercept the output power $P_0$ at $f_1$. The output power $P_0$ is directly proportional to the amplitude of the input signal while the output power $P_{2(f_1+f_2)}$ is directly proportional to the fourth power of the input signal, at lower power levels. Thus, on logarithmic scales, the output power versus input power would be straight lines with a slope corresponding to the order of the response, i.e., the response at $f_1$ will have a slope of 1 and the response at $2(f_1+f_2)$ will have a slope of 4, as shown in Figure B1.

Assume a two-tone signal is

$$s_{in}(t)=A\cos\left(2\pi f_c t\right)+A\cos\left(2\pi f_2 t\right) \quad \text{(B1)}$$

where $A$ is the amplitude of the tones. By inserting Equation (A5) into Taylor series Equation (4) with weak nonlinearity assumption, we have:

$$\begin{aligned}s_{out}(t)=&\,a_2A^2+\frac{9}{4}a_4A^4+\left(a_1A+\frac{9}{4}a_3A^3\right)\cos\left(2\pi f_1 t\right)\\&+\left(a_1A+\frac{9}{4}a_3A^3\right)\cos\left(2\pi f_2 t\right)\\&+\frac{1}{4}a_3A^3\cos\left(6\pi f_1 t\right)+\frac{1}{4}a_3A^3\cos\left(6\pi f_2 t\right)\\&+\frac{1}{8}a_4A^4\cos\left(8\pi f_1 t\right)+\frac{1}{8}a_4A^4\cos\left(8\pi f_2 t\right)\\&+\left(\frac{1}{2}a_2A^2+2a_4A^4\right)\cos\left(4\pi f_1 t\right)\\&+\left(\frac{1}{2}a_2A^2+2a_4A^4\right)\cos\left(4\pi f_2 t\right)\\&+\left(a_2A^2+3a_4A^4\right)\cos\left[2\pi\left(f_1+f_2\right)t\right]\\&+\left(a_2A^2+3a_4A^4\right)\cos\left[2\pi\left(f_1-f_2\right)t\right]\\&+\frac{3}{4}a_3A^3\cos\left[2\pi\left(f_1+2f_2\right)t\right]\\&+\frac{3}{4}a_3A^3\cos\left[2\pi\left(f_1-2f_2\right)t\right]\\&+\frac{3}{4}a_3A^3\cos\left[2\pi\left(2f_1+f_2\right)t\right]\\&+\frac{3}{4}a_3A^3\cos\left[2\pi\left(2f_1-f_2\right)t\right]\\&+\frac{1}{2}a_4A^4\cos\left[2\pi\left(3f_1+f_2\right)t\right]\\&+\frac{1}{2}a_4A^4\cos\left[2\pi\left(3f_1-f_2\right)t\right]\\&+\frac{1}{2}a_4A^4\cos\left[2\pi\left(f_1+3f_2\right)t\right]\\&+\frac{1}{2}a_4A^4\cos\left[2\pi\left(f_1-3f_2\right)t\right]\\&+\frac{3}{4}a_4A^4\cos\left[2\pi\left(2f_1+2f_2\right)t\right]\\&+\frac{3}{4}a_4A^4\cos\left[2\pi\left(2f_1-2f_2\right)t\right]\end{aligned} \quad \text{(B2)}$$

From (A6), we have:

$$P_0=10\times\log\left[\left(\frac{a_1A}{\sqrt{2}}\right)^2\frac{10^3}{R}\right]\ \text{dBm} \quad \text{(B3)}$$

$$P_{4(f_1+f_2)}=10\times\log\left[\left(\frac{\frac{3}{4}a_4A^4}{\sqrt{2}}\right)^2\frac{10^3}{R}\right]\ \text{dBm} \quad \text{(B4)}$$

By the definition of $IP_4$, $P_0=P_{2(f_1+f_2)}$. By comparing Equations (A7) and (A8), we can obtain the theoretical amplitude $A$

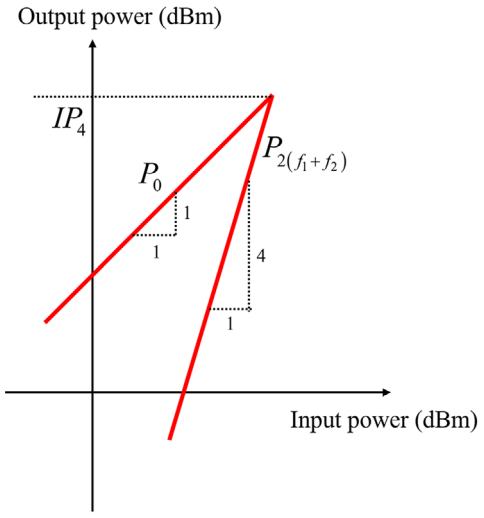


**FIGURE B1** Illustration of $IP_4$

at $IP_4$ as:

$$\mathcal{A}\,(\text{at}\quad IP_4) = \left|\frac{4a_1}{3a_4}\right|^{\frac{1}{3}} \tag{B5}$$

Then, by substituting Equation (A9) into either Equation (A7) or Equation (A8), we have:

$$IP_4 = 10 \times \log\left[\left(\frac{2a_1^8}{9a_4^2}\right)^{\frac{1}{3}}\frac{10^3}{R}\right]\ \text{dBm} \tag{B6}$$

After changing the $IP_4$ scale from dBm to dB and assuming $R = 1$, we have:

$$IP_4 = 10 \times \log\left(\frac{2a_1^8}{9a_4^2}\right)^{\frac{1}{3}} \tag{B7}$$

$$10^{\frac{3IP_4}{10}} = \frac{2}{9}\frac{a_1^8}{a_4^2} \tag{B8}$$

With $a_1 = 10^{G/20}$ from [10],

$$a_4^2 = \frac{2}{9}a_1^8 10^{\frac{-3IP_4}{10}} = \frac{2}{9}10^{\frac{2G}{5}-\frac{3IP_4}{10}} \tag{B9}$$